

Supporting Information

Electrosynthesis of a RuAg alloy for an efficiently alkaline hydrogen evolution reaction

Tzung-Wen Chiou*, Jia-Min Shen

Department of Chemistry, Tunghai University, Taichung 407224, Taiwan

Email: twchiou@thu.edu.tw

Experimental section

Chemicals. RuCl_3 (99 %) was purchased from Thermo scientific. AgNO_3 (99.0 %) and potassium citrate tribasic monohydrate (99 %) were bought from Acros Organics. $\text{CuSO}_4 \cdot 5\text{H}_2\text{O}$ (99 %) and KOH (99 %) were purchased from Duksan. HNO_3 was bought from Union Chemical Works LTD (Taiwan). Platinum on carbon (20 wt. % Pt/C, Pt on an activated carbon support) and Nafion® perfluorinated resin solution (5 wt. % in lower aliphatic alcohols and water, contains 15-20% water) were bought from Sigma-Aldrich. All chemicals were used directly without further purification. Ultrapure water (18.2 M Ω) used in the experiments was supplied by a Millipore System (Direct-Q® 3).

Electrode Preparation. The electrodeposition was carried out with a standard three-electrode electrochemical cell containing glassy carbon disk (surface area: 0.0707 cm²), a graphite rod (L 100 mm, diam. 3 mm) and a saturated calomel electrode (SCE) as the working, auxiliary and reference electrodes, respectively. In order to the physical characterizations, electrodepositions on graphite plate electrodes as the working electrode were performed. The electrolyte solution of RuAg alloy was prepared; RuCl_3 (0.0083 g, 0.04 mmol), AgNO_3 (0.0340 g, 0.2 mmol), potassium citrate tribasic monohydrate (3.2441 g, 0.01 mol) and 1.0 M HNO_3 (0.2 mL) were dissolved in 20 mL DI water. The electrolyte solution of Ru NP was prepared; RuCl_3 (0.0083 g, 0.04 mmol), potassium citrate tribasic monohydrate (3.2441 g, 0.01 mol) and 1.0 M HNO_3 (0.2 mL) were dissolved in 20 mL DI water. The electrolyte solution of Ag NP was prepared; AgNO_3 (0.0340 g, 0.2 mmol), potassium citrate tribasic monohydrate (3.2441 g, 0.01 mol) and 1.0 M HNO_3 (0.2 mL) were dissolved in 20 mL DI water. All materials were prepared through controlled potential electrolysis at -1.544 V (vs SCE) for 3000 s at ambient temperature. After deposition, the materials by careful rinse with water were

directly used for electrochemistry tests. 20 wt.% Pt/C (20 mg) was dispersed in a 5 mL mixture solution containing 0.5 mL 5% Nafion solution and 4.5 mL methanol, followed by sonication for 30 min to obtain a homogeneous catalyst ink. The catalyst ink was loaded on the surfaces of the glassy carbon disk electrode to achieve 1.0 mg cm^{-2} .

Physical characterization. Powder X-ray diffraction (pXRD) data were obtained using a Rigaku MiniFlex X-ray Powder Diffractometer with a Cu K- α radiation source in the range $2\theta = 5\text{-}100^\circ$. Scanning electron microscopy (SEM) images were obtained with a JSM-6510 microscope (JEOL) equipped. The morphologies of samples were characterized on a transmission electron microscope (TEM, JEOL JEM-1400, Japan) by dropping sample solutions on Cu grids. HRTEM images were obtained with a JEM-2010 microscope (JEOL) equipped. X-ray photoelectron spectroscopy (XPS) spectra were collected on a ULVAC-PHI XPS spectrometer equipped with a monochromatized 1486.6 eV Al K α X-ray line source directed 45° with respect to the sample surface. The spectra were registered at a base pressure of $<5 \times 10^{-10}$ torr. Low-resolution survey scans were acquired with a 100 μm spot size between the binding energies of 1-1100 eV. High-resolution scans with a resolution of 0.2 eV were collected between 453-503 (for Ru) and 362-382 (for Ag) eV.

Electrochemical measurements. All electrochemical experiments were performed with a CH Instrument 621b potentiostat. Fundamental electrochemical testing was carried out, consisting of samples as the working electrode, a graphite rod (L 100 mm, diam. 3 mm) auxiliary electrode and a saturated calomel electrode (SCE) reference electrode. All potentials reported in this paper were converted from vs SCE to vs reversible hydrogen electrode (RHE). $\text{RHE} = \text{SCE} + 0.244 + 0.059 \times \text{pH}$. In all experiments, the iR compensation was performed by CHI model 621b software. The

linear sweep voltammetry (LSV) curves were obtained in 1.0 M KOH at a scan rate of 2 mV/s. Tafel slopes were calculated using the Polarization curves by plotting overpotential against $\log(\text{current density})$. Controlled potential electrolysis (CPE) experiments were conducted in 1.0 M KOH stirred constantly. The auxiliary electrode in CPE cell was separated from the solution of the working electrode by a medium-porosity sintered-glass frit. The electrochemically active surface area (ECSA) was evaluated in terms of double-layer capacitance. Cyclic voltammogram (CV) scans were conducted in static solution by sweeping the potential from the more positive to negative potential and back at 8 different scan rates: 20, 40, 60, 80 and 100 mV s^{-1} . The capacitance was determined from the tenth cyclic voltammetry curve of each scan rate. The electrochemical double-layer capacitance, C_{DL} , as given by $i_c = \nu C_{DL}$ (i_c : current density from CV, ν : scan rate). The specific capacitance for a flat surface is generally found to be in the range of 20-60 mF cm^{-2} . We used a value of 40 mFcm^{-2} in the following calculations of the electrochemical active surface area. The electrochemical impedance spectroscopy (EIS) measurements were carried out in a frequency range of 0.1 Hz to 100 kHz with an amplitude of 5 mV at an overpotential of 30 mV. The curve fitting was performed by Zview2 software.

ICP-MS experiment. ICP-MS was performed on a Thermo Scientific™ Element 2™ (Germany). Dry sample was dissolved in concentrated HNO_3 .

Determinations of Faradaic Efficiency and TOF. Quantification of the produced H_2 gas was performed by gas chromatography (Chromatec-Crystal 9000) equipped with a micropacked column (ShinCarbon ST #19808, Restek) and thermal conductivity detector (TCD). Helium was used as the carrier gas. Calibration curves were built by the injection of the known amounts of pure H_2 . The amounts of H_2 dissolved in the

solution were corrected by the Henry's law ($K_H = 7.8 \times 10^{-4}$ mol/atm·L for H₂).

$$\text{Faradaic efficiency (FE \%)} = (V_{\text{H}_2}/24.5) \times 100\% / (Q_{\text{CPE}}/2F)$$

where V_{H_2} is the volume (L) of H₂ gas by GC detection, Q_{CPE} is the charge (C) during CPE and F is the Faraday constant.

The TOF (s⁻¹) can be calculated with the following equation: $\text{TOF} = I/2Fn$ where I is the current of LSV curve, F is the Faraday constant and n is the number of active sites (mol).

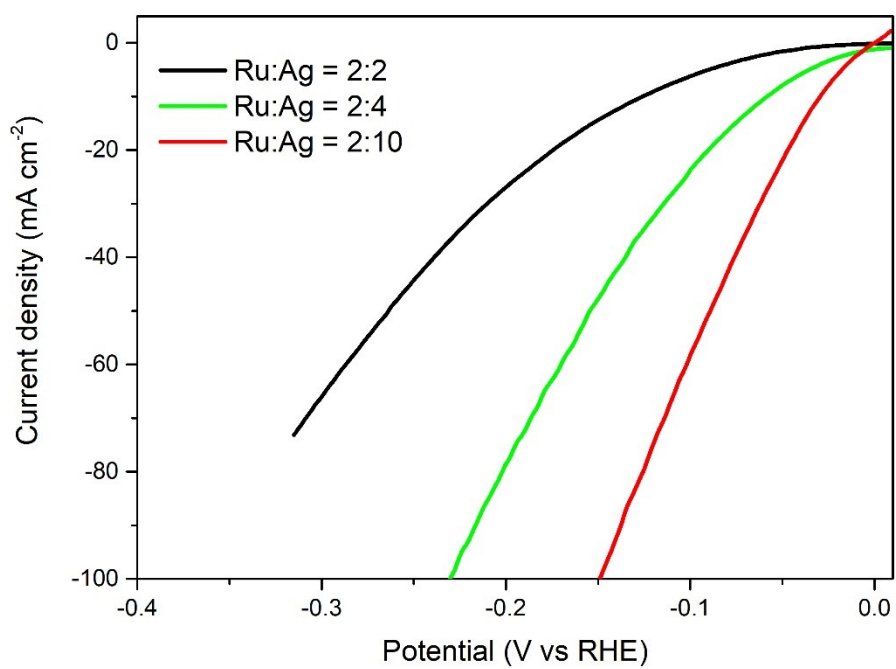


Figure S1. LSV curves of varying ratio RuAg alloy.

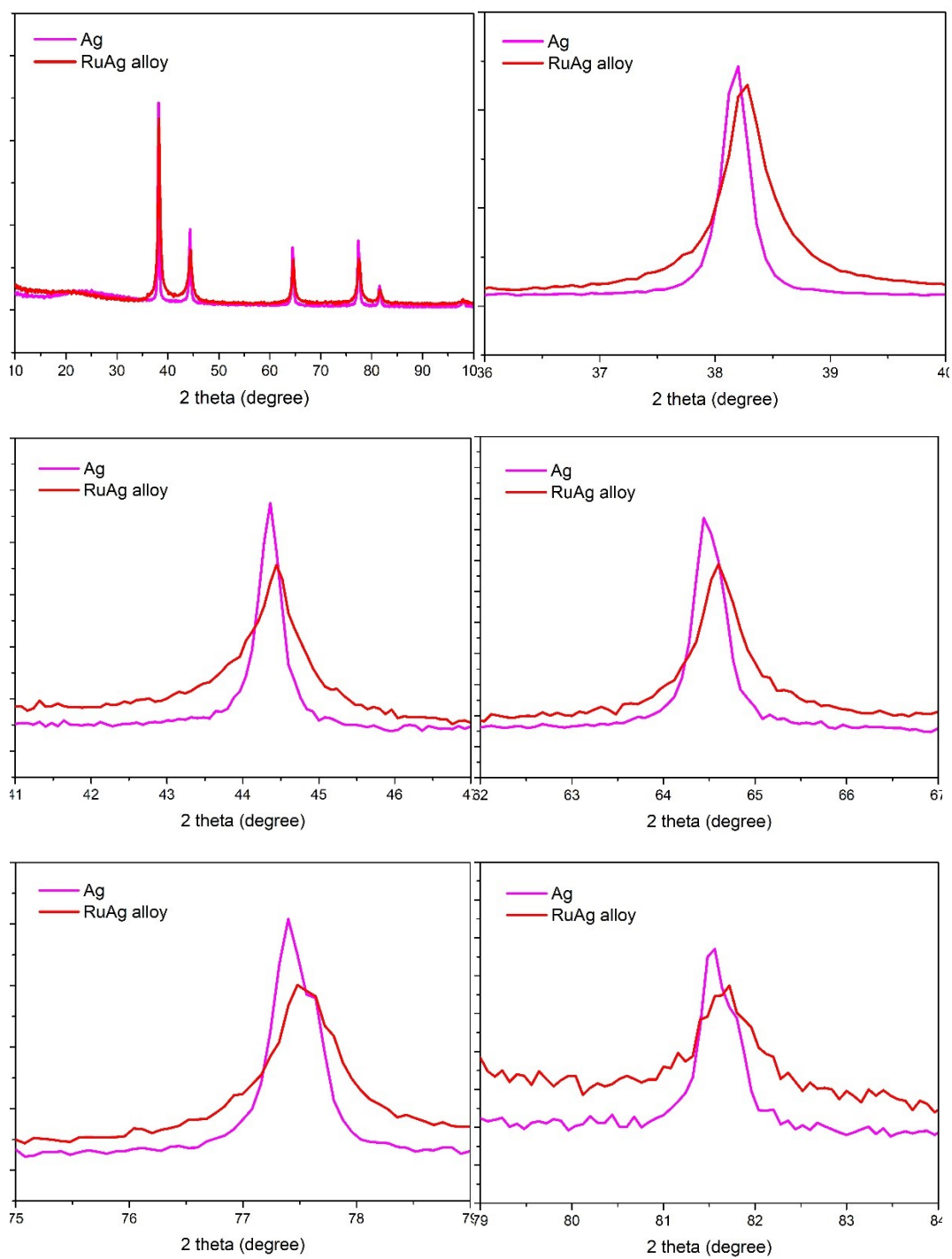
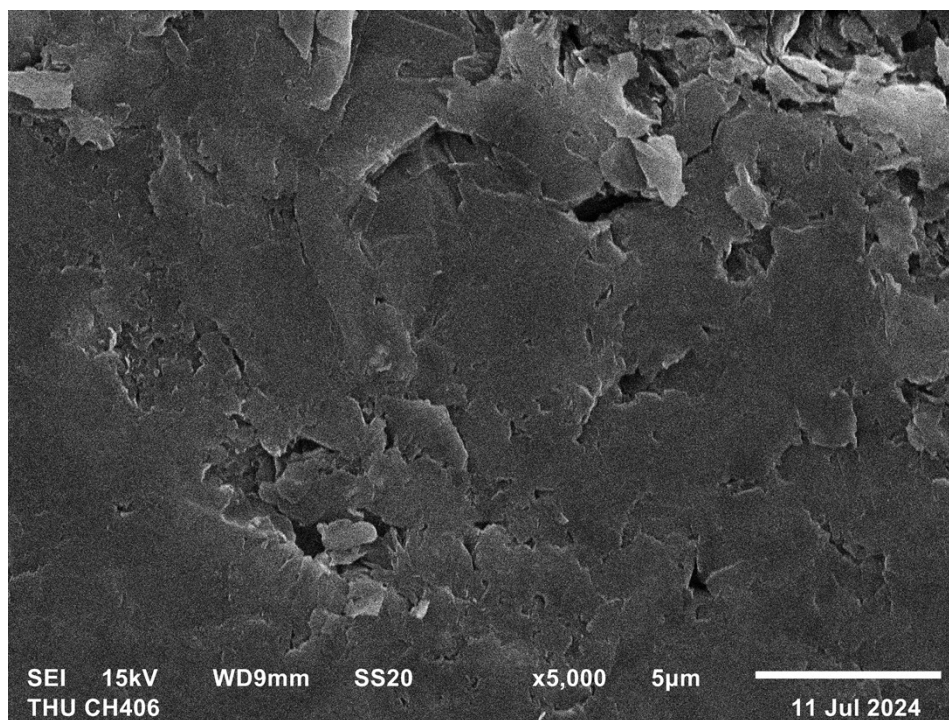


Figure S2. XRD patterns of RuAg alloy and Ag NP.

a.



b.

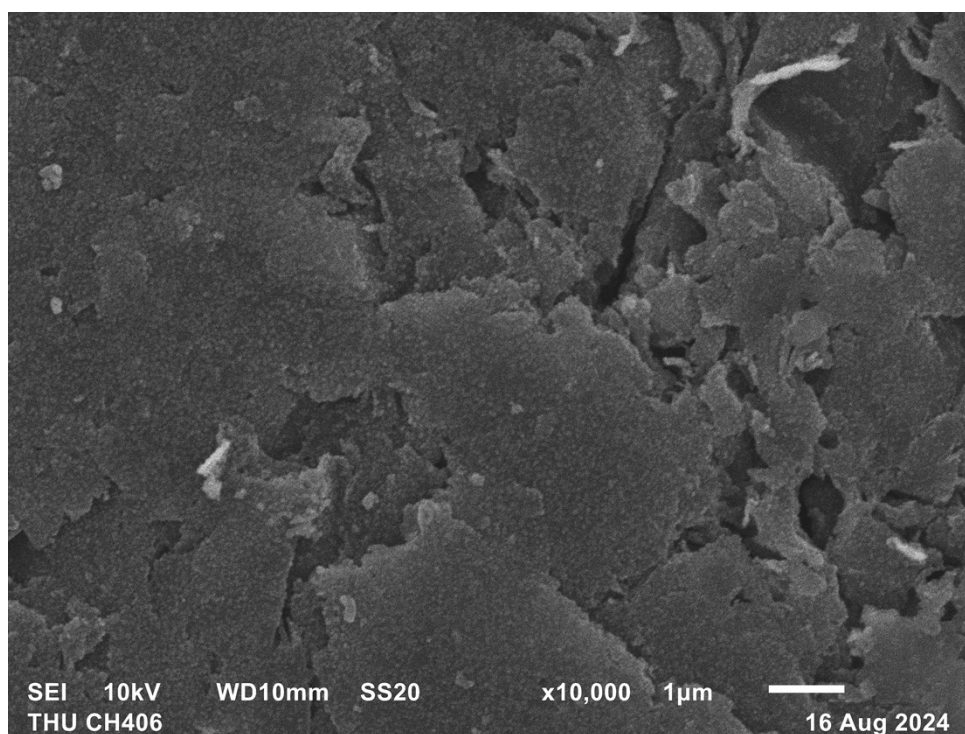


Figure S3. SEM images of (a) fresh graphite and (b) Ru NP.

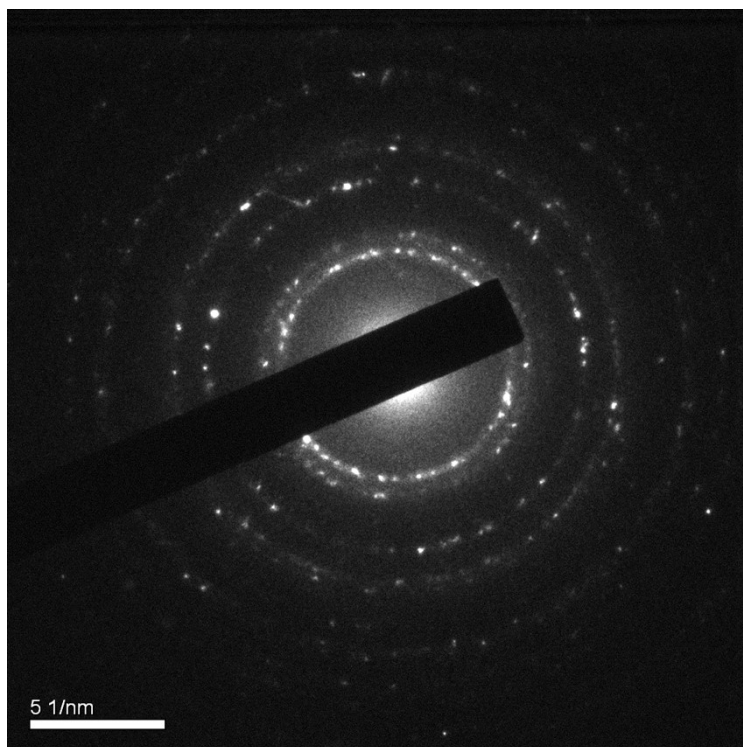


Figure S4. Selected-area electron diffraction pattern of RuAg alloy.

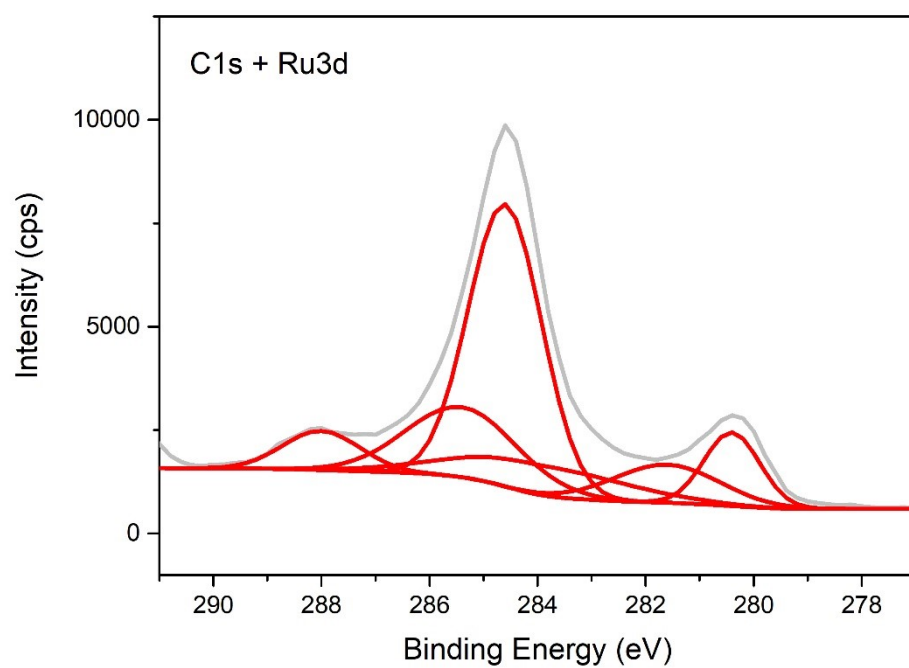


Figure S5. C 1s and Ru 3d XPS spectrum of RuAg alloy.

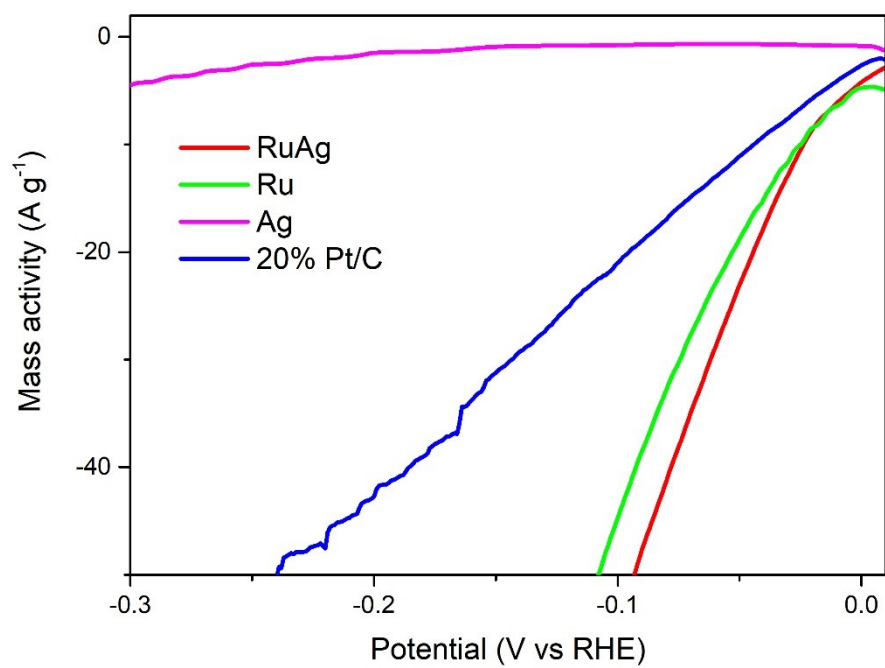


Figure S6. Mass activity of RuAg alloy, Ru NP, Ag NP, and 20% Pt/C.

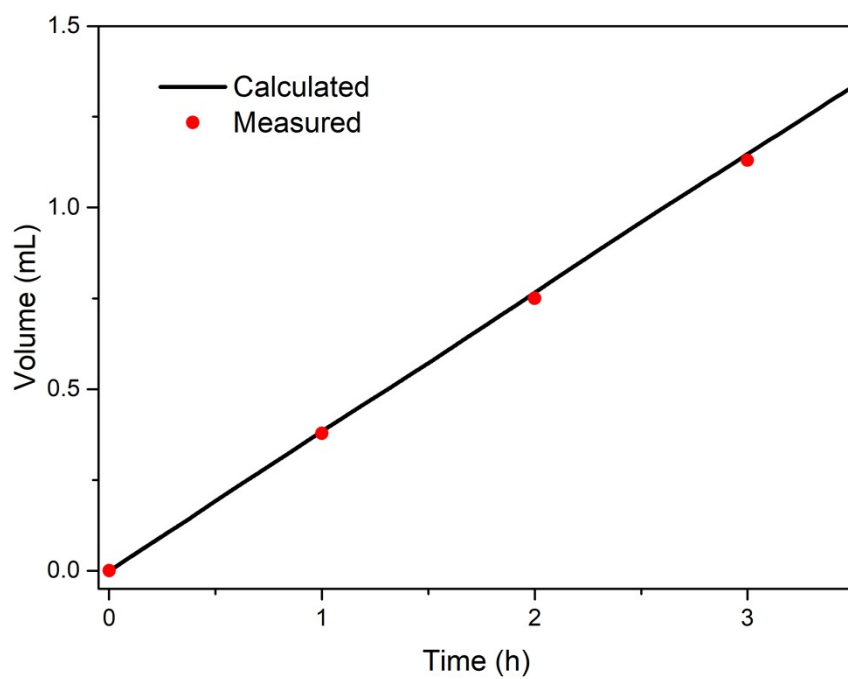


Figure S7. Electrocatalytic Faradaic efficiency of hydrogen production over RuAg alloy at the current density of 10 mA cm⁻².

a.

b.

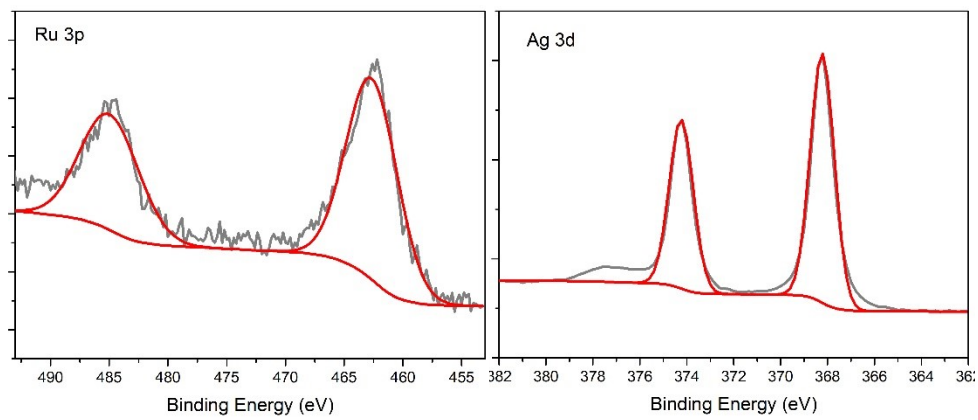


Figure S8. XPS spectra of RuAg alloy after CPE.

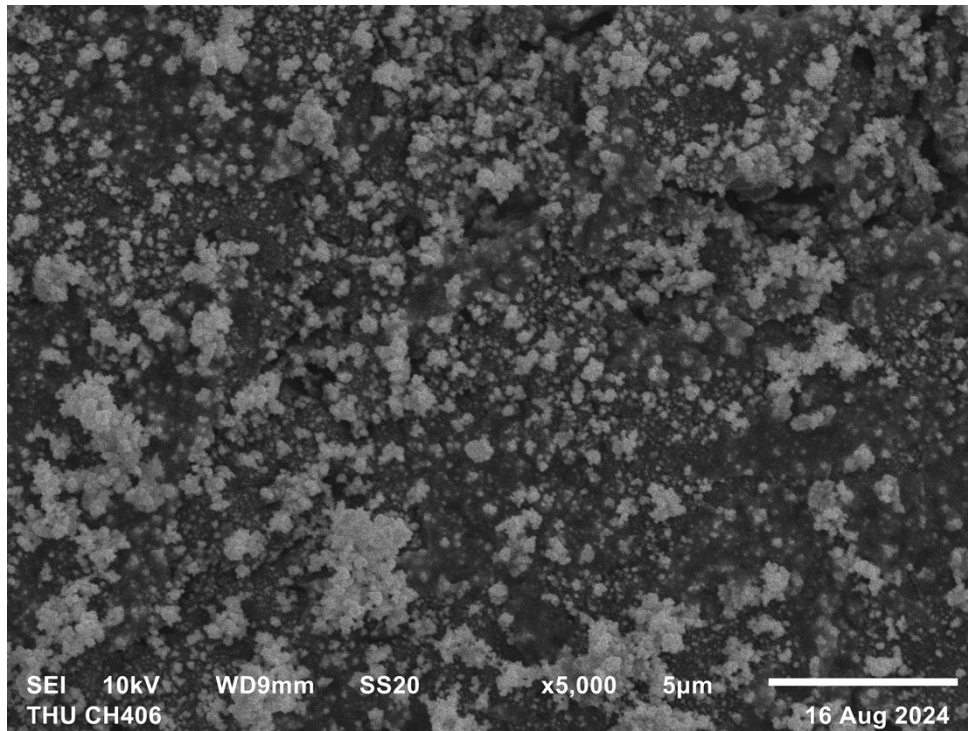


Figure S9. SEM image of RuAg alloy after CPE.

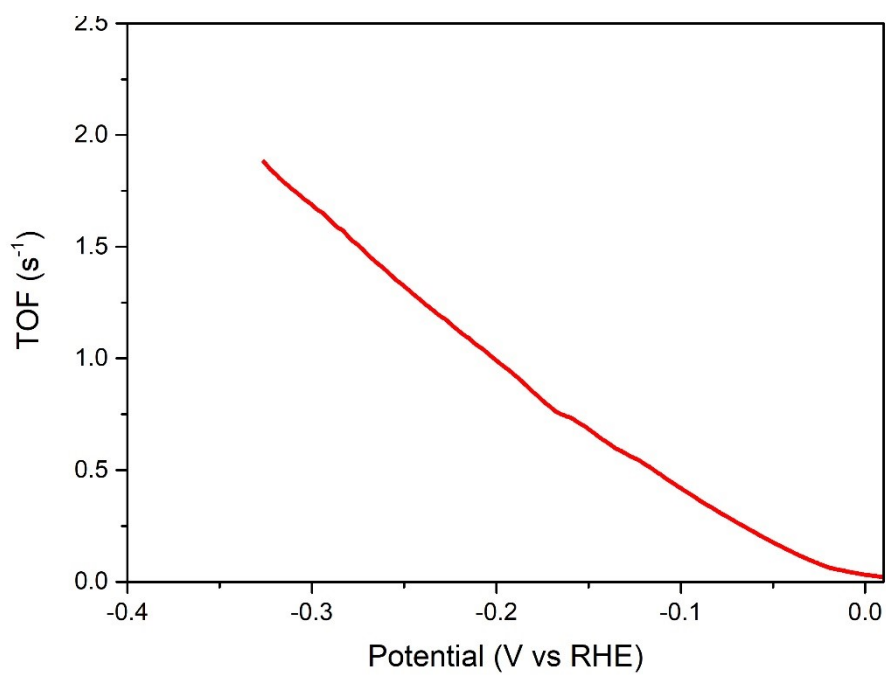
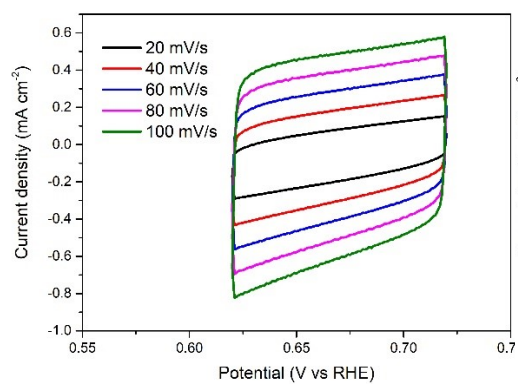
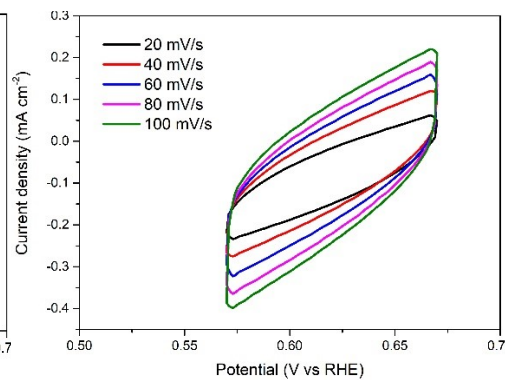


Figure S10. TOF of RuAg alloy in 1.0 M KOH.

a.



b.



c.

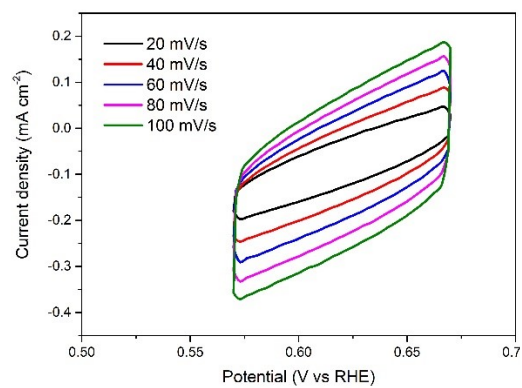


Figure S11. CV curves of (a) RuAg alloy, (b) Ru NP and (c) Ag NP in 1.0 M KOH at different scan rates of 20, 40, 60, 80 and 100 mV s^{-1} .

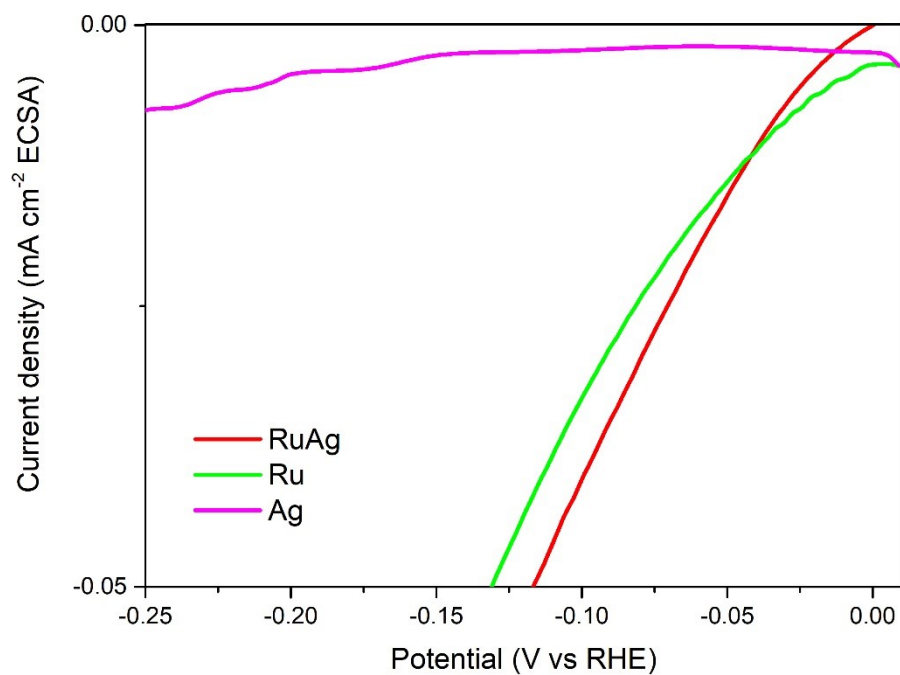


Figure S12. LSV curves from Fig. 3a normalized to the electrochemical active surface area (ECSA).